JACS
JOURNAL OF THE AMERICAN CHEMICAL SOCIETY
Communication
Cite This: J. Am. Chem. Soc. 2017, 139, 16442-16445
pubs.acs.org/JACS

Micellar Thrombin-Binding Aptamers: Reversible Nanoscale Anticoagulants

Alexander Roloff,*[,†] Andrea S. Carlini,[†] Cassandra E. Callmann,[†] and Nathan C. Gianneschi*[,†,⊥,§]

[†]Department of Chemistry & Biochemistry, [⊥]Materials Science and Engineering, University of California, San Diego, La Jolla, California 92093, United States

[§]Department of Chemistry, Materials Science and Engineering, Biomedical Engineering, Northwestern University, Evanston, Illinois 60208, United States

Supporting Information

ABSTRACT: Aptamers are nucleic acid-based ligands that exhibit promising features including specific and reversible target binding and inhibition. Aptamers can function as anticoagulants if they are directed against enzymes of the coagulation cascade. However, they typically suffer from nucleolytic digestion and fast clearance from the bloodstream. We present thrombin-binding aptamer amphiphiles that self-assemble into nanoscale polymeric micelles with a densely functionalized aptamer-displaying corona. We show that these micellar aptamers retain their native secondary structure in a crowded environment and are stabilized against degradation by nucleases in human serum. Moreover, they are effective inhibitors of human plasma clotting *in vitro*. The inhibitory effect can be rapidly reversed by complementary nucleic acids that break the aptamers' secondary structure upon hybridization. Compared to free aptamers, the increased molecular weight and size of the overall assembly promotes extended blood circulation times *in vivo*.

Downloaded via NORTHWESTERN UNIV on July 12, 2018 at 15:31:58 (UTC).
See https://pubs.acs.org/sharingguidelines for options on how to legitimately share published articles.

Aptamers represent a fascinating class of nucleic acid-based ligands.[1] The rich sequence space of DNA and RNA allows to select aptamers for a multitude of proteins, which are particularly interesting as therapeutic targets.[2] For example, aptamers directed against enzymes of the coagulation cascade can function as potent anticoagulants.[3] However, aptamers typically suffer from fast degradation by nucleases present in serum.[4] Moreover, rapid renal clearance severely hampers *in vivo* applications,[5] which limits their use in clinical settings.[6] Strategies exist for increasing the bioavailability and stability of aptamers. For example, the VEGF antagonist pegaptanib is a highly modified RNA aptamer containing PEG chains, 2′-ribose modifications and inverted 3′-thymidine caps.[7] Whereas pegaptanib is injected intravitreally to treat age-related macular degeneration, other targets such as enzymes involved in blood coagulation circulate in the bloodstream and call for intravenous administration of aptamers.

The three-dimensional (3D) arrangement of nucleic acids on nanomaterial surfaces can mediate stabilization against nucleolytic degradation[8] and, in combination with PEGylation, prolonged retention in blood circulation[9] without modifying the ribose backbone. Nanoparticle (NP) surface-displayed aptamers have been utilized as targeting ligands or sensors,[10] but combined approaches where they also function as medical effectors are rare.[11] In these examples, aptamer-decorated gold NPs were employed, whose loading capacity is limited by the metal scaffold and the thiol-conjugation chemistry. Moreover, *in vivo* toxicity of metallic particle cores[12] and oligonucleotide displacement by thiolated biomolecules[13] can be problematic.

Purely organic, soft NPs can self-assemble from functionalized building blocks such as nucleic acid−lipid[14] and −polymer[8b,c,15] conjugates. Here, the nucleic acid density on the nanomaterial surface is governed by the packing of the hydrophobic portions of amphiphiles into vesicular membranes and micelle cores. Furthermore, inert linkages between nucleic acids and hydrophobes can provide stability against nucleophilic displacement. In particular, aptamer-lipid-based nanomaterials have been studied for their self-assembly and cellular recognition properties as well as payload release.[14] However, lipid-derived NPs contain fluidic bilayers or cores and are therefore transient in nature. Moreover, very little is known about nuclease resistance and *in vivo* blood circulation properties of such self-assembled materials. Thus, the development of soft organic aptamer-based nanostructures that feature increased stability in biological fluids and extended blood circulation times in comparison to free aptamers is important with respect to potential therapeutic applications.

In this work, we introduce DNA−aptamer polymer amphiphiles that self-assemble into uniformly sized spherical NPs (**DAPA-NPs**, Figure 1). We show that the surface-displayed aptamers retain their secondary structure within the compact micelle coronas. Moreover, we demonstrate that micellar aptamers can specifically bind and inhibit their target within biological fluids including human plasma. Importantly, the dense display on micelle coronas stabilizes the aptamers against degradation by nucleases, and the increased size helps extend blood circulation times *in vivo* as examined in mice.

We focused on thrombin-binding DNA aptamers (TBAs)[3a,16] as a proof of principle system. TBAs adopt antiparallel G-quadruplexes that mediate binding to and inhibition of thrombin. The synthesis of DNA−aptamer polymer amphiphiles was accomplished by conjugating a support-bound amino-modified TBA to a carboxy-terminated polymer of (*N*-benzyl)-5-norbornene-exo-2,3-dicarboximide[8b] with an average chain length of 19 (see the Supporting Information for details). The polymer features a high glass transition temperature above the

Received: July 25, 2017
Published: November 14, 2017

© 2017 American Chemical Society

DOI: 10.1021/jacs.7b07799
J. Am. Chem. Soc. 2017, 139, 16442−16445

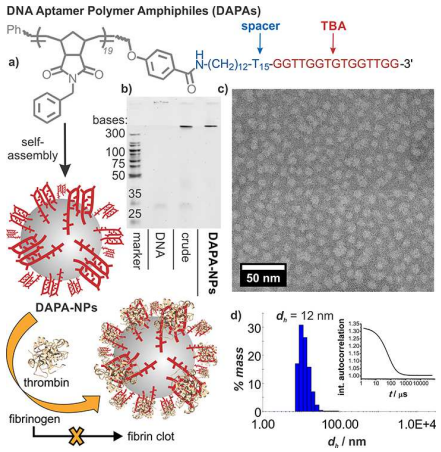

Figure 1. (a) Polymer–DNA–aptamer conjugates self-assemble into **DAPA-NPs** that display thrombin-binding aptamers (TBAs) on their coronas. Binding to thrombin inhibits fibrinogen processing and delays blood clotting. **DAPA-NPs** were characterized via (b) PAGE (before/after SEC purification), (c) TEM and (d) DLS. See Supporting Information for additional characterization.

boiling point of water,[17] which facilitates kinetic trapping and stability of the resulting NPs. A 5′-T_{15}-spacer was included between the quadruplex-forming sequence and the polymer to facilitate aptamer-folding in the crowded micelle coronas (Figure 1a). Upon cleavage and deprotection, the amphiphiles spontaneously assembled into nanoscale micelles, driven by exclusion of water from the polymeric core. **DAPA-NPs** were purified by SEC, after which PAGE verified the absence of unconjugated DNA (Figure 1b). TEM and DLS measurements revealed spherical particles with dry state and hydrodynamic diameters around 10 nm (Figure 1c,d). The ζ-potential was −24 mV. Aggregation numbers of ca. 60 amphiphiles per micelle were calculated from SLS experiments (Table S1). This translates into occupied surface areas of ca. 8 nm^2 per aptamer, which represents a high density when compared to previously reported gold NPs.[11a]

Initially, we examined whether the 3D-arrangement of aptamers on micelle coronas would mediate resistance against nucleases (Figure 2). In these experiments, a 3′-T^{FAM}-modified DNA sequence was incorporated to facilitate read-out. According to PAGE analysis, **DAPA-NPs** were significantly less prone to degradation by DNase I than the unconjugated TBA. For example, 89 and 100% of free TBA were cleaved after incubation for 2 and 24 h, whereas the same sequence displayed on **DAPA-NPs** resulted in only 17 and 43% cleavage, respectively

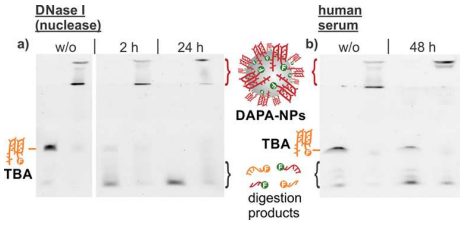

Figure 2. PAGE analysis after incubating **DAPA-NPs** or free TBAs a) with DNase I (0.1 u·μL^{-1}) or b) in 50 vol % human serum (5 μM DNA, 37 °C). The controls (w/o) were incubated without DNase or serum for 24 and 48 h, respectively.

(Figure 2a and S1a). Stabilization was also observed in human serum, that contains the whole variety of nucleases present in blood. Only 13 and 21% of the micellar aptamers were digested after incubation for 24 and 48 h at 37 °C. The unconjugated TBA gave rise to ca. 3-fold higher cleavage yields (44 and 60%, Figures 2b and S1b). We note that some aggregation might occur during prolonged incubation with nucleases or in serum, as the intensity of the slow migrating band increased over time. Slow nuclease processing of DNA displayed on nanomaterial surfaces has been explained by steric hindrance and high local salt concentrations that can inhibit these enzymes.[8]

CD spectroscopy can reveal insights into whether the micellar DNA folds into a biologically active secondary structure, thus mimicking native sequence behavior (Figure 3). The CD spectra

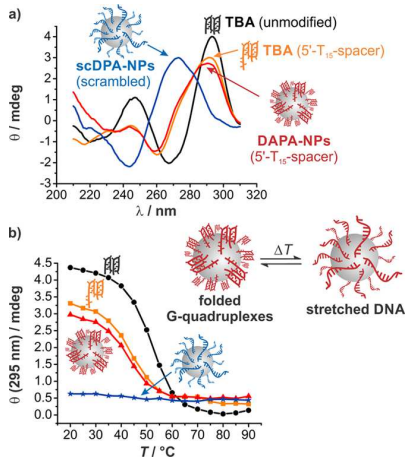

Figure 3. (a) CD spectra and (b) thermal unfolding of G-quadruplexes of free TBAs and **DAPA-NPs**/**scDPA-NPs**. Conditions: 5 μM DNA in buffer (10 mM KH_2PO_4, 150 mM KCl, pH 7.4).

of **DAPA-NPs** and free TBAs both bearing a T_{15}-spacer are virtually identical and reflect features of an antiparallel G-quadruplex (Figure 3a, compared to the unmodified TBA).[18] This suggests that aptamer folding is not affected within the densely functionalized micelle coronas. Contrarily, **scDPA-NPs** displaying a scrambled sequence produced a distinct spectrum, confirming that this DNA adopts a different secondary structure. **DAPA-NPs** lacking a spacer or bearing an additional 3′-T^{FAM} produced less pronounced signals (Figure S2a). This implies that the spacer is crucial for quadruplex-folding within the crowded environment, and that the dye-labeled nucleotide on the 3′-terminus impedes quadruplex folding.

The temperature-dependency of the G-quadruplex-associated signal at 295 nm followed a sigmoidal curve for the spacer-modified **DAPA-NPs** and free TBAs (Figure 3b). Although the melting temperature (T_m) decreased by 6–7 °C compared to the unmodified TBA (T_m = 51 °C), both predominantly adopt a quadruplex conformation at 37 °C. In contrast, no temperature-dependency was observed for the scrambled **scDPA-NPs** and **DAPA-NPs** lacking a spacer (Figure S2b). An additional 3′-T^{FAM} significantly reduced the signal intensities as well as the T_m to 37 °C.

Next, we explored whether **DAPA-NPs** could delay the clotting of human plasma by inhibiting thrombin (Figure 4). During clotting, the thrombin-catalyzed formation of a fibrin network increases the viscosity of the solution, which can be

DOI: 10.1021/jacs.7b07799
J. Am. Chem. Soc. 2017, 139, 16442–16445

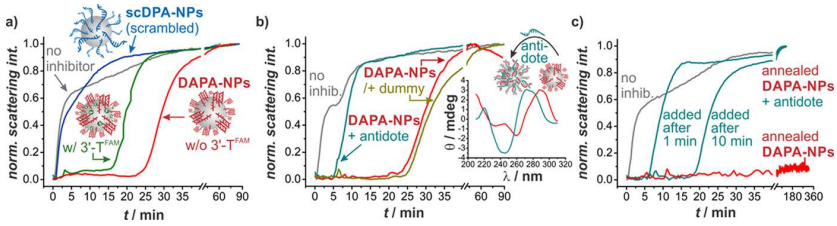

Figure 4. Kinetics of plasma clotting (determined by light scattering, λ_{sc} = 658 nm) in absence and presence of (a) **DAPA-NPs** (with or without 3′-T^{FAM} label) or scrambled **scDPA-NPs**, (b) **DAPA-NPs** without or with 1.5 equiv antidote or dummy DNA added after 1 min (CD spectra as inset (conditions as in Figure 3)) or (c) annealed **DAPA-NPs** without or with 1.5 equiv antidote added after 1 or 10 min. Conditions: citrate-deactivated human plasma (50 vol %) + **DAPA-NPs**/**scDPA-NPs** (1 μM DNA) in buffer at 37 °C, clotting was initiated by adding 1 u·mL^{-1} thrombin and 25 mM $CaCl_2$.

monitored via light scattering. In absence of thrombin inhibitors, the scattering intensity reached its half-maximum value after 3 min (Figure 4a). In presence of **DAPA-NPs**, however, this value was shifted to 30 min. This 10-fold delay demonstrates that micellar aptamers bind and inhibit their specific target in a pool of various other plasma proteins. **DAPA-NPs** labeled with 3′-T^{FAM} were less effective and delayed plasma clotting only 6.7-fold. This corroborates results from CD spectroscopy, that accounted for less stable quadruplexes on these micelles, and contrasts a previous study that reported enhanced efficacies for TBAs bearing 3′-extensions.[19] Importantly, thrombin inhibition by scrambled **scDPA-NPs** via nonspecific electrostatic interactions was not observed. The effect was dose-dependent (Figure S3), and the spacer length influenced the anticoagulytic potential of **DAPA-NPs** (Figure S4). A shorter T_5-spacer was significantly less efficient than the T_{15}-spacer, whereas extension to 25 nucleotides did not lead to further improvement. Presumably, a certain length is sufficient to facilitate G-quadruplex annealing within the micelle coronas.

The target-affinity of aptamers is a direct result of their specific 3D structure. Hence, aptamers can be neutralized by hybridization to complementary nucleic acids that disrupt their folding pattern.[20] Indeed, upon addition of a complementary antidote DNA, the CD spectrum of **DAPA-NPs** indicated a switch from G-quadruplex to duplex DNA (Figure 4b (inset) and S5). Accordingly, when the antidote was added to human plasma containing **DAPA-NPs**, the inhibitory effect was rapidly reversed within minutes, and plasma clotting was reinstalled to its original rate (Figure 4b). A noncomplementary dummy DNA was ineffective, demonstrating sequence specificity. The efficacy of **DAPA-NPs** could be significantly improved by incorporating a simple annealing step (5 min 85 °C, slow cooling to 37 °C), which supports accurate G-quadruplex folding. In the presence of annealed **DAPA-NPs**, plasma clotting was now completely abolished for at least 5 h (Figure 4c, we observed similar efficiencies with free TBA, Figure S6). Of note, the antidote still neutralized the annealed **DAPA-NPs** in a time-dependent fashion.

We quantified the anticoagulant potencies of **DAPA-NPs** in human plasma and directly compared them to unmodified TBAs by measuring the clinically relevant activated partial thromboplastin and prothrombin times (APTT, PT, Figure 5a,b). We found that **DAPA-NPs** delayed the APTT from 28 to 188 s (6.7-fold), whereas free TBAs only caused a 3.5-fold delay (98 s). This superior efficacy could be caused by multivalence effects (local effective aptamer concentrations on micelle surfaces of ca. 100 mM were calculated, Table S1). However, some nonspecific inhibition was observed with scrambled **scDPA-NPs** (67 s). We speculate that this may be caused by calcium-binding to the

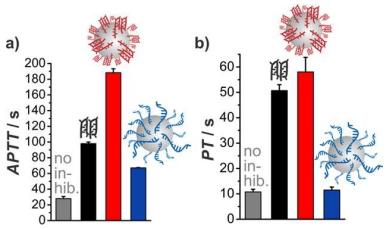

Figure 5. (a) Activated partial thromboplastin time (APTT) and (b) prothrombin time (PT) of human plasma clotting in absence and presence of free TBAs or **DAPA-NPs**/**scDPA-NPs**.

negatively charged micelle surface, which would reduce the availability of this cofactor. **DAPA-NPs** also significantly delayed the PT from 11 to 58 s, which was comparable to free TBAs (51 s). In this assay, **scDPA-NPs** had no significant effect (11 s).

One of the major drawbacks of aptamers is their fast clearance rate when injected in the bloodstream.[5] We assessed whether the increased size and nuclease resistance of micellar aptamers would have a beneficial effect on the blood circulation time (Figure 6).

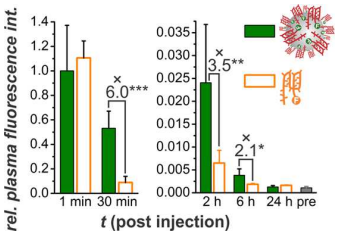

Figure 6. Blood clearance of fluorescein-labeled **DAPA-NPs** vs free TBAs: relative fluorescence intensities of mice plasma before (pre) and after injection of fluorescein-labeled **DAPA-NPs** or free TBAs (n = 3, p = 0.01 (***), 0.11 (**), 0.14 (*)).

Fluorescein-labeled **DAPA-NPs** and free TBAs were injected into mice via the tail vein. Blood was collected via the retro-orbital plexus at several time points and the plasma was analyzed for fluorescence. At 1 min post-injection, both groups showed similar plasma fluorescence intensities, verifying comparable initial blood concentrations. After 30 min, plasma fluorescence of mice that were injected with **DAPA-NPs** still retained 53% of the initial value. In contrast, a 6-fold lower value was measured for mice injected with free TBAs (8%). Thus, the assembly of aptamer−polymer amphiphiles into micellar NPs clearly led to a substantial prolongation of the blood circulation time. Higher plasma fluorescence intensities were also measured after 2 and 6 h, albeit with lower statistical significance, until reaching background levels after 24 h. Note that the fluorophore is

DOI: 10.1021/jacs.7b07799
J. Am. Chem. Soc. 2017, 139, 16442−16445

located on the outermost 3′-nucleotide in the micelle corona. Therefore, any measured signal must come from intact nanomaterials, as cleaved DNA fragments would be cleared rapidly from circulation and lead to loss of dye. It is conceivable that expanding the particle size beyond the 10 nm regime by increasing the length of the polymeric segment may further increase the circulation time of micellar aptamers, as renal filtration, for example, is known to be less pronounced for larger nanomaterials.[21] Of note, prolonged blood circulation was achieved without relying on common shielding strategies such as PEGylation.[9,22,23]

In this work, we introduce thrombin-binding aptamer–polymer amphiphiles that assemble into quasi-single-entity micellar nanoparticles (**DAPA-NPs**) with uniform size and shape. Incorporating spacer nucleotides facilitates folding into the desired G-quadruplexes, and the high-density display on micelle coronas mediates stability against degradation by nucleases in buffer and in human serum. **DAPA-NPs** are efficient clotting inhibitors in human plasma that can be rapidly neutralized by the addition of complementary oligonucleotides. **DAPA-NPs** are equally or more efficient in blood clotting assays when compared to free aptamers, and benefit from extended blood circulation times *in vivo* in mice. We postulate that formulating nucleic acid amphiphiles into nanoscale micelles may prove effective in extending the *in vivo* availability of aptamers and other nucleic acid-based effectors in general, including RNA.

■ ASSOCIATED CONTENT

Supporting Information

The Supporting Information is available free of charge on the ACS Publications website at DOI: 10.1021/jacs.7b07799.

Detailed descriptions of synthetic and experimental procedures, characterization of compounds and additional data and images (PDF)

■ AUTHOR INFORMATION

Corresponding Authors

*aroloff@ucsd.edu

*nathan.gianneschi@northwestern.edu

ORCID

Nathan C. Gianneschi: 0000-0001-9945-5475

Notes

The authors declare no competing financial interest.

■ ACKNOWLEDGMENTS

We acknowledge support from the National Science Foundation (NSF, DMR-1710105), and from the German Academic Exchange Service (DAAD) through a fellowship to A.R. within the postdoc program.

■ REFERENCES

(1) (a) Tuerk, C.; Gold, L. *Science* **1990**, *249*, 505. (b) Ellington, A. D.; Szostak, J. W. *Nature* **1990**, *346*, 818. (c) Ellington, A. D.; Szostak, J. W. *Nature* **1992**, *355*, 850.

(2) (a) Famulok, M.; Hartig, J. S.; Mayer, G. *Chem. Rev.* **2007**, *107*, 3715. (b) Nimjee, S. M.; Rusconi, C. P.; Sullenger, B. A. *Annu. Rev. Med.* **2005**, *56*, 555.

(3) (a) Bock, L. C.; Griffin, L. C.; Latham, J. A.; Vermaas, E. H.; Toole, J. J. *Nature* **1992**, *355*, 564. (b) Rusconi, C. P.; Scardino, E.; Layzer, J.; Pitoc, G. A.; Ortel, T. L.; Monroe, D.; Sullenger, B. A. *Nature* **2002**, *419*, 90. (c) Heckel, A.; Mayer, G. *J. Am. Chem. Soc.* **2005**, *127*, 822. (d) Nimjee, S. M.; Rusconi, C. P.; Harrington, R. A.; Sullenger, B. A. *Trends Cardiovasc. Med.* **2005**, *15*, 41.

(4) Tolle, F.; Mayer, G. *Chem. Sci.* **2013**, *4*, 60.

(5) Griffin, L. C.; Tidmarsh, G. F.; Bock, L. C.; Toole, J. J.; Leung, L. L. K. *Blood* **1993**, *81*, 3271.

(6) Keefe, A. D.; Pai, S.; Ellington, A. *Nat. Rev. Drug Discovery* **2010**, *9*, 537–550.

(7) (a) Lee, J.-H.; Canny, M. D.; De Erkenez, A.; Krilleke, D.; Ng, Y.-S.; Shima, D. T.; Pardi, A.; Jucker, F. *Proc. Natl. Acad. Sci. U. S. A.* **2005**, *102*, 18902. (b) Vinores, S. A. *Nat. Rev. Drug Discovery* **2006**, *5*, 123.

(8) (a) Seferos, D. S.; Prigodich, A. E.; Giljohann, D. A.; Patel, P. C.; Mirkin, C. A. *Nano Lett.* **2009**, *9*, 308. (b) Rush, A. M.; Thompson, M. P.; Tatro, E. T.; Gianneschi, N. C. *ACS Nano* **2013**, *7*, 1379. (c) Tan, X.; Li, B. B.; Lu, X.; Jia, F.; Santori, C.; Menon, P.; Li, H.; Zhang, B.; Zhao, J. J.; Zhang, K. *J. Am. Chem. Soc.* **2015**, *137*, 6112.

(9) Chinen, A. B.; Ferrer, J. R.; Merkel, T. J.; Mirkin, C. A. *Bioconjugate Chem.* **2016**, *27*, 2715.

(10) (a) Farokhzad, O. C.; Jon, S.; Khademhosseini, A.; Tran, T.-N. T.; Lavan, D. A.; Langer, R. *Cancer Res.* **2004**, *64*, 7668. (b) Dhar, S.; Gu, F. X.; Langer, R.; Farokhzad, O. C.; Lippard, S. J. *Proc. Natl. Acad. Sci. U. S. A.* **2008**, *105*, 17356. (c) Zheng, D.; Seferos, D. S.; Giljohann, D. A.; Patel, P. C.; Mirkin, C. A. *Nano Lett.* **2009**, *9*, 3258–3261.

(11) (a) Shiang, Y.-C.; Huang, C.-C.; Wang, T.-H.; Chien, C.-W.; Chang, H.-T. *Adv. Funct. Mater.* **2010**, *20*, 3175. (b) Shiang, Y.-C.; Hsu, C.-L.; Huang, C.-C.; Chang, H.-T. *Angew. Chem., Int. Ed.* **2011**, *50*, 7660.

(12) (a) Alkilany, A. M.; Murphy, C. J. *J. Nanopart. Res.* **2010**, *12*, 2313. (b) Wu, X. A.; Choi, C. H. J.; Zhang, C.; Hao, L.; Mirkin, C. A. *J. Am. Chem. Soc.* **2014**, *136*, 7726. (c) Chompoosor, A.; Saha, K.; Ghosh, P. S.; Macarthy, D. J.; Miranda, O. R.; Zhu, Z.-J.; Arcaro, K. F.; Rotello, V. M. *Small* **2010**, *6*, 2246–2249.

(13) Letsinger, R. L.; Elghanian, R.; Viswanadham, G.; Mirkin, C. A. *Bioconjugate Chem.* **2000**, *11*, 289–291.

(14) (a) Wu, Y. R.; Sefah, K.; Liu, H. P.; Wang, R. W.; Tan, W. H. *Proc. Natl. Acad. Sci. U. S. A.* **2010**, *107*, 5. (b) Pearce, T. R.; Waybrant, B.; Kokkoli, E. *Chem. Commun.* **2014**, *50*, 210. (c) Waybrant, B.; Pearce, T. R.; Kokkoli, E. *Langmuir* **2014**, *30*, 7465. (d) Liang, C.; Guo, B.; Wu, H.; Shao, N.; Li, D.; Liu, J.; Dang, L.; Wang, C.; Li, H.; Li, S.; Lau, W. K.; Cao, Y.; Yang, Z.; Lu, C.; He, X.; Au, D. W. T.; Pan, X.; Zhang, B.-T.; Lu, C.; Zhang, H.; Yue, K.; Qian, A.; Shang, P.; Xu, J.; Xiao, L.; Bian, Z.; Tan, W.; Liang, Z.; He, F.; Zhang, L.; Lu, A.; Zhang, G. *Nat. Med.* **2015**, *21*, 288.

(15) (a) Alemdaroglu, F. E.; Ding, K.; Berger, R.; Herrmann, A. *Angew. Chem., Int. Ed.* **2006**, *45*, 4206. (b) Chien, M.-P.; Rush, A. M.; Thompson, M. P.; Gianneschi, N. C. *Angew. Chem., Int. Ed.* **2010**, *49*, 5076. (c) Rush, A. M.; Nelles, D. A.; Blum, A. P.; Barnhill, S. A.; Tatro, E. T.; Yeo, G. W.; Gianneschi, N. C. *J. Am. Chem. Soc.* **2014**, *136*, 7615. (d) Kwak, M.; Herrmann, A. *Chem. Soc. Rev.* **2011**, *40*, 5745. (e) Schnitzler, T.; Herrmann, A. *Acc. Chem. Res.* **2012**, *45*, 1419. (f) Zhang, C.; Hao, L.; Calabrese, C. M.; Zhou, Y.; Choi, C. H. J.; Xing, H.; Mirkin, C. A. *Small* **2015**, *11*, 5360. (g) Jia, F.; Lu, X.; Tan, X.; Zhang, K. *Chem. Commun.* **2015**, *51*, 7843.

(16) Mayer, G.; Rohrbach, F.; Pötzsch, B.; Müller, J. *Haemostaseologie* **2011**, *31*, 258.

(17) Barnhill, S. A.; Bell, N. C.; Patterson, J. P.; Olds, D. P.; Gianneschi, N. C. *Macromolecules* **2015**, *48*, 1152.

(18) Paramasivan, S.; Rujan, I.; Bolton, P. H. *Methods* **2007**, *43*, 324.

(19) Buff, M. C. R.; Schäfer, F.; Wulffen, B.; Müller, J.; Pötzsch, B.; Heckel, A.; Mayer, G. *Nucleic Acids Res.* **2010**, *38*, 2111.

(20) Rusconi, C. P.; Roberts, J. D.; Pitoc, G. A.; Nimjee, S. M.; White, R. R.; Quick, G.; Scardino, E.; Fay, W. P.; Sullenger, B. A. *Nat. Biotechnol.* **2004**, *22*, 1423.

(21) Longmire, M.; Choyke, P. L.; Kobayashi, H. *Nanomedicine (London, U. K.)* **2008**, *3*, 703.

(22) Dai, Q.; Walkey, C.; Chan, W. C. W. *Angew. Chem., Int. Ed.* **2014**, *53*, 5093.

(23) Verhoef, J. J. F.; Anchordoquy, T. J. *Drug Delivery Transl. Res.* **2013**, *3*, 499.

DOI: 10.1021/jacs.7b07799
J. Am. Chem. Soc. 2017, 139, 16442–16445